Geometric scaling and QCD evolution

J. Kwieciński
H. Niewodniczański Institute of Nuclear Physics, Kraków, Poland

A. M. Staśto
H. Niewodniczański Institute of Nuclear Physics, Kraków, Poland
and INFN Sezione di Firenze, Via G. Sansone 1, 50019 Sesto Fiorentino (FI), Italy

(Received 4 March 2002; published 29 July 2002)

We study the impact of the QCD Dokshitzer-Gribov-Lipatov-Altarelli-Parisi (DGLAP) evolution on the geometric scaling of gluon distributions that is expected to hold at small x within the saturation models. With this aim we solve the DGLAP evolution equations with the initial conditions provided along the critical line $Q^2=Q_s^2(x)$ with $Q_s^2(x)\sim x^{-\lambda}$ and satisfying geometric scaling. Both fixed and running coupling cases are studied. We show that in the fixed coupling case the geometric scaling at low x is stable against the DGLAP evolution for sufficiently large values of the parameter λ, and in the double logarithmic approximation of the DGLAP evolution this happens for $\lambda \geqslant 4N_c\alpha_s/\pi$. In the running coupling case geometric scaling is found to be approximately preserved at very small x. The residual geometric scaling violation in this case can be approximately factored out and the corresponding form factor controlling this violation is found.

DOI: 10.1103/PhysRevD.66.014013 PACS number(s): 12.38.Bx

I. INTRODUCTION

Perturbative QCD predicts a very strong power-law rise of the gluon density $xg(x,Q^2)$ in the limit $x\to 0$, where, as usual, x denotes the momentum fraction carried by the gluon and Q^2 is the scale at which the distribution is probed. This strong rise can eventually violate unitarity and so it has to be tamed by screening effects. Those screening effects are provided by multiple parton interactions which lead to the nonlinear terms in the Balitskiĭ-Fadin-Kuraev-Lipatov (BFKL) and/or Dokshitzer-Gribov-Lipatov-Attarelli-Parissi (DGLAP) equations [1–13]. These nonlinear terms reduce the growth of gluon distributions and generate instead parton saturation at sufficiently small values of x and/or Q^2 [1–20].

The increase of the gluon distribution and emergence of the saturation effects imply similar properties of the measurable quantities which are driven by the gluon, such as the deep inelastic structure function $F_2(x,Q^2)$. This can be most clearly seen in the dipole picture of deep inelastic scattering in which the virtual photon-proton total cross section $\sigma_{\gamma^* p}(x,Q^2)$ [$\sigma_{\gamma^* p}(x,Q^2)\sim F_2(x,Q^2)/Q^2$)] is linked with the cross section $\sigma_{dp}(x,r)$ describing the interaction of the $q\bar{q}$ color dipole with the proton, where r denotes the transverse size of the dipole [3,21–23]. The dipole-proton cross section is determined by the gluon distribution in the proton and in leading order approximation we just have $\sigma_{dp}(x,r)\sim\alpha_s(1/r^2)r^2xg(x,1/r^2)$. An increase and/or saturation of the gluon distribution in the small x limit implies a similar increase and/or saturation of the dipole-proton cross section and of the cross section $\sigma_{\gamma^* p}(x,Q^2)$.

The successful description of all inclusive and diffractive deep inelastic data at the DESY of collider HERA by the saturation model [22] suggests that the screening effects might become important in the energy regime probed by present colliders. The important property of the dipole cross section which holds in this model is its geometric scaling, i.e., dependence upon the single variable $\tau=r^2Q_s^2(x)$, where $Q_s(x)$ is the saturation scale. This leads to the geometric scaling of $\sigma_{\gamma^* p}(x,Q^2)$ itself, i.e., $\sigma_{\gamma^* p}(x,Q^2)=f(Q^2/Q_s^2(x))$, which is well supported by the experimental data from HERA [24]. Geometric scaling of the dipole cross section should imply similar scaling of the quantity $\alpha_s(Q^2)xg(x,Q^2)/Q^2$. This type of scaling is also found to be an intrinsic property of the nonlinear evolution equations [6,8,11–20]. It turns out that for equations of the type

$$\frac{\partial\phi(x,k)}{\partial\ln(1/x)}=\bar{\alpha}_sK\otimes\phi-\bar{\alpha}_s\phi^2(x,k),\qquad\left(\bar{\alpha}_s\equiv\frac{N_c\alpha_s}{\pi}\right),\tag{1}$$

where K is a linear evolution kernel (for example of the BFKL type), there exists a region in x and k space such that

$$\phi(x,k)=\phi(Q_s^2(x)/k^2)\quad\text{for}\quad k^2<Q_s^2(x).\tag{2}$$

For example in the case of the Balitsky-Kovchegov equation [11,12], where K is the BFKL kernel, the saturation scale $Q_s^2(x)$ has been found to have a general powerlike dependence on x, $Q_s^2(x)=Q_0^2x^{-\lambda}$. The coefficient λ, which is approximately equal to $4\bar{\alpha}_s$ in this case, is then a universal quantity and does not depend on the initial conditions for the evolution [16–20].

The main purpose of this paper is to analyze possible compatibility of this scaling with the DGLAP evolution equations. It is expected that the nonlinear shadowing effects should be weak in the region ''to the right'' of the critical line defined by the saturation scale $Q_s^2(x)$, i.e., for $Q^2>Q_s^2(x)$ (see Fig. 1). In order to study the possible impact of the DGLAP evolution we shall therefore assume geometric scaling parametrization along the critical line and inspect the structure of the solution of the DGLAP equation with those

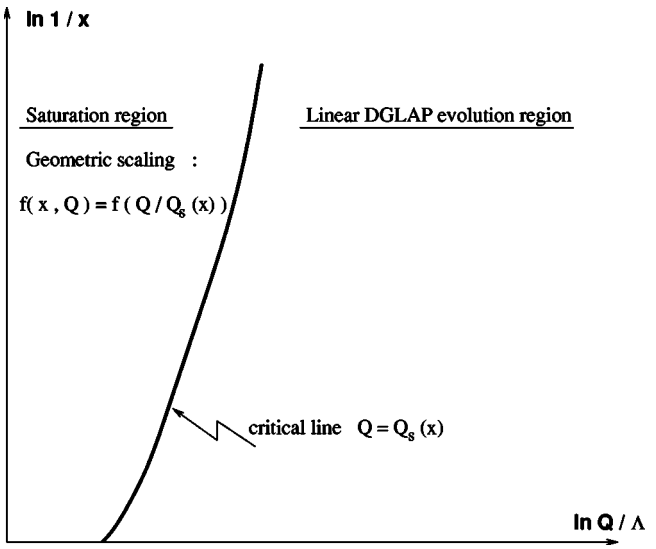

FIG. 1. Phase diagram in $(\ln 1/x, \ln Q/\Lambda)$ space. Thick line is the critical line $Q^2=Q_s^2(x)$ which divides the saturation scaling regime (to the left) and the linear DGLAP regime (to the right).

initial conditions. This way of providing the initial conditions along the critical line $Q^2=Q_s^2(x)$ rather than at $Q^2=Q_0^2$ with x the independent reference scale Q_0^2 is the characteristic feature of the saturation effects [1].

The content of our paper is as follows. In the next section we give a semianalytical insight into the solution of the DGLAP equation with the starting distributions provided along the critical line. We study separately the fixed and running coupling cases. In Sec. III we present a numerical analysis of our solutions and finally in Sec. IV we give our conclusions.

II. SOLUTION OF THE DGLAP EQUATIONS FROM THE STARTING DISTRIBUTIONS PROVIDED ALONG THE CRITICAL LINE

We wish to understand the possible effects of the DGLAP evolution on the geometric scaling at low x. This scaling means that certain quantities controlling deep inelastic scattering at low x, like the dipole-proton cross section $\sigma_{dp}(x,r=1/Q)$ or the virtual photon-proton cross section $\sigma_{\gamma^* p}$, which are in principle functions of two variables, depend upon the single variable $Q/Q_s(x)$. The saturation scale $Q_s(x)$, which also specifies the critical line, increases with decreasing x:

$$Q_s^2(x)=Q_0^2 x^{-\lambda}. \tag{3}$$

Let us assume these following.

(1) For $Q^2<Q_s^2(x)$ the linear evolution is strongly perturbed by nonlinear effects which generate geometric scaling for the dipole cross section $\sigma_{dp}(x,r=1/Q)$ and for related quantities.

(2) Geometric scaling for the dipole cross section implies geometric scaling for $\alpha_s(Q^2)xg(x,Q^2)/Q^2$, where $g(x,Q^2)$ denotes the gluon distribution. This follows from the leading order (LO) relation between the dipole cross section and the gluon distribution, i.e., $\sigma(x,r^2)\sim r^2\alpha_s(1/r^2)xg(x,1/r^2)$.

(3) Geometric scaling for $\alpha_s(Q^2)xg(x,Q^2)/Q^2$ holds at the boundary $Q^2=Q_s^2(x)$.

(4) For $Q^2>Q_s^2(x)$ the nonlinear screening effects can be neglected and evolution of parton densities is governed by the DGLAP equations.

We wish to study possible effects of the DGLAP evolution upon the geometric scaling in the region $Q^2>Q_s^2(x)$ after solving the linear DGLAP evolution equations starting from the gluon distribution satisfying this scaling and defined along the critical line $Q_s^2(x)$ (see point 3 above). We shall discuss the fixed and running coupling cases separately.

A. Fixed coupling case

Let us consider the standard leading order evolution of the gluon distribution $xg(x,Q^2)$:

$$\frac{\partial xg(x,Q^2)}{\partial \ln(Q^2/\Lambda^2)}=\frac{\alpha_s}{2\pi}\int_x^1\frac{dz}{z}P_{gg}(z)xg(x/z,Q^2), \tag{4}$$

where, as usual, P_{gg} is the gluon-gluon splitting function. For simplicity we have neglected possible contributions of the quark distributions. In the moment space this equation has the following form:

$$\frac{\partial g_\omega(Q^2)}{\partial\ln(Q^2/\Lambda^2)}=\frac{\alpha_s}{2\pi}\gamma_{gg}(\omega)g_\omega(Q^2), \tag{5}$$

where we have defined the Mellin transform to be

$$g_\omega(Q^2)=\int_0^1 dx x^\omega g(x,Q^2), \tag{6}$$

and the gluon anomalous dimension is defined as

$$\gamma_{gg}(\omega)=\int_0^1 dz z^\omega P_{gg}(z). \tag{7}$$

The solution of Eq. (5) is straightforward and given by

$$g_\omega(Q^2)=g_0(\omega)\left(\frac{Q^2}{Q_0^2}\right)^{(\alpha_s/2\pi)\gamma_{gg}(\omega)}. \tag{8}$$

We will now seek the equation for the moment function $g_0(\omega)$ using the following initial condition:

$$\frac{\alpha_s}{2\pi}xg(x,Q^2=Q_s^2(x))=\frac{\alpha_s}{2\pi}r^0x^{-\lambda}, \tag{9}$$

where $Q_s^2(x)$ is given by Eq. (3). The parameter r^0 specifies the normalization of the gluon distribution along the critical line. This boundary condition follows from the geometric scaling condition of the dipole-proton cross section $\sigma_{dp}(r=1/Q,x)$ which is proportional to $\alpha_s xg(x,Q^2)/Q^2$.

In order to find solution for $g_0(\omega)$ we use the inverse Mellin transform

$$xg(x,Q^2)=\frac{1}{2\pi i}\int d\omega x^{-\omega}g_\omega(Q^2), \tag{10}$$

where the integration contour should be located to the right of the singularities of $g_\omega(Q^2)$ in the ω plane. Inserting in Eq. (10) the DGLAP solution (8) for $g_\omega(Q^2)$, we get

$$xg(x,Q^2)=\frac{1}{2\pi i}\int d\omega x^{-\omega} g_0(\omega)\left(\frac{Q^2}{Q_0^2}\right)^{(\alpha_s/2\pi)\gamma_{gg}(\omega)}. \tag{11}$$

We now set $Q^2=Q_s^2(x)$ with the saturation scale $Q_s^2(x)$ defined by Eq. (3), and require the geometric scaling initial condition along the critical line $Q^2=Q_s^2(x)$ [see Eq. (9)]. From Eqs. (3), (9), and (11) we get

$$\frac{1}{2\pi i}\int d\omega g_0(\omega) x^{-\omega-\lambda(\alpha_s/2\pi)\gamma_{gg}(\omega)}=r^0 x^{-\lambda}. \tag{12}$$

This equation can be regarded as the equation for the function $g_0(\omega)$, i.e., for the moment of the gluon distribution at the (x independent) scale Q_0^2. In order to solve this equation we take the moment of both sides of Eq. (12), i.e. we integrate both sides of this equation over dx for $0<x<1$ with the weight x^{ω_1-1} and get

$$\frac{1}{2\pi i}\int d\omega \frac{g_0(\omega)}{[\omega_1-\omega-\lambda(\alpha_s/2\pi)\gamma_{gg}(\omega)]}=\frac{r^0}{\omega_1-\lambda}. \tag{13}$$

We now change the integration variables

$$z=\omega+\lambda\frac{\alpha_s}{2\pi}\gamma_{gg}(\omega), \tag{14}$$

which after inversion specifies the function $\omega(z)$. Equation (13) in the new variable z then takes the following form:

$$\frac{1}{2\pi i}\int dz \frac{d\omega(z)}{dz}\frac{g_0(\omega(z))}{(\omega_1-z)}=\frac{r^0}{\omega_1-\lambda}. \tag{15}$$

We can easily perform the contour integration in Eq. (15) and get

$$\left.\frac{d\omega(z)}{dz}\right|_{z=\omega_1} g_0(\omega(z=\omega_1))=\frac{r^0}{\omega_1-\lambda}. \tag{16}$$

We still need to solve this equation for $g_0(\omega)$ and in order to do this we write

$$\omega_1=\omega+\lambda\frac{\alpha_s}{2\pi}\gamma_{gg}(\omega), \tag{17}$$

and finally from Eq. (16) we obtain

$$g_0(\omega)=\left[1+\lambda\frac{\alpha_s}{2\pi}\frac{d\gamma_{gg}(\omega)}{d\omega}\right]\times\frac{r^0}{[\omega+\lambda(\alpha_s/2\pi)\gamma_{gg}(\omega)-\lambda]}, \tag{18}$$

which defines the solution for $g_0(\omega)$.

In what follows it is convenient to use directly the redefined function $\tilde{g}_0(z)$,

$$\tilde{g}_0(z)\equiv\frac{d\omega(z)}{dz}g_0(\omega(z)), \tag{19}$$

where from Eq. (16) we see that

$$\tilde{g}_0(z)=\frac{r^0}{z-\lambda}. \tag{20}$$

The solution of the DGLAP equation with the initial condition specified by Eq. (9) then reads

$$xg(x,Q^2)=\frac{1}{2\pi i}\int dz x^{-z}\tilde{g}_0(z)\left(\frac{Q^2}{Q_s^2(x)}\right)^{(\alpha_s/2\pi)\gamma_{gg}(\omega(z))} \tag{21}$$

where the integration contour is located to the right of the singularities of $\tilde{g}_0(z)$ and of $\omega(z)$. If the leading singularity is a pole of $\tilde{g}_0(z)$ at $z=\lambda$ then the leading contribution to $xg(x,Q^2)$ at small x is given by

$$xg(x,Q^2)\simeq r^0 x^{-\lambda}\left(\frac{Q^2}{Q_s^2(x)}\right)^{(\alpha_s/2\pi)\gamma_{gg}(\omega_0)}, \tag{22}$$

where

$$\omega_0=\omega(\lambda). \tag{23}$$

It should be noted that ω_0 defines the position of the pole of $g_0(\omega)$. In general we have $\omega_0\leqslant\lambda$. From Eq. (22) we get the following leading small x behavior for the gluon density $(\alpha_s/2\pi)xg(x,Q^2)/Q^2$:

$$\frac{\alpha_s}{2\pi}\frac{xg(x,Q^2)}{Q^2}\simeq\frac{r^0}{Q_0^2}\left(\frac{\alpha_s}{2\pi}\right)\left(\frac{Q^2}{Q_s^2(x)}\right)^{(\alpha_s/2\pi)\gamma_{gg}(\omega_0)-1}, \tag{24}$$

which respects the geometric scaling, i.e., is a function of only one combined variable $Q^2/Q_s^2(x)$. Violation of this scaling by the contribution of the (branch point) singularity of $\omega(z)$ is a nonleading effect at low x.

The requirement that the pole of $\tilde{g}^0(z)$ at $z=\lambda$ is the leading singularity imposes certain constraints upon λ. In general they are difficult to find exactly since the inversion of Eq. (14) cannot be performed analytically when using the complete form of $\gamma_{gg}(\omega)$. The analytic solution of Eq. (14) is possible, however, in the double logarithmic approximation in which $\gamma_{gg}(\omega)=\gamma_{gg}^{DL}(\omega)$, where

$$\gamma_{gg}^{DL}(\omega)=\frac{2N_c}{\omega} \tag{25}$$

is the most singular in $\omega\to 0$ part of the gluon anomalous dimension $\gamma_{gg}(\omega)$. In this approximation we get

$$\omega(z)=\frac{z+\sqrt{z^2-4\bar{\alpha}_s\lambda}}{2}, \tag{26}$$

where

$$\bar{\alpha}_s = \frac{N_c \alpha_s}{\pi}. \tag{27}$$

We also have

$$\omega_0 = \frac{\lambda + \sqrt{\lambda^2 - 4\bar{\alpha}_s \lambda}}{2}. \tag{28}$$

The condition that the pole of $\tilde{g}^0(z)$ at $z=\lambda$ is the leading singularity, i.e. that it is located to the right of the branch-point singularity of $\omega(z)$ at $z = 2\sqrt{\bar{\alpha}_s \lambda}$, gives the following constraint upon the parameter λ:

$$\lambda \geqslant 4\bar{\alpha}_s. \tag{29}$$

For $\lambda < 4\bar{\alpha}_s$ the leading singularity is the branch point of $\omega(z)$ at $z = 2\sqrt{\bar{\alpha}_s \lambda}$ and the geometric scaling becomes violated.

It may be interesting to confront our results for the fixed coupling with the properties of the exact solution of the nonlinear Balitsky-Kovchegov equation [20]. In this case geometric scaling holds for $Q^2 \leqslant Q_s^2(x)$ and the nonlinear effects can be neglected for $Q^2 > Q_s^2(x)$. The parameter λ specifying the critical line is, however, not an independent quantity and depends upon the (fixed) coupling α_s. In the double logarithmic approximation it is given by $\lambda = 4\bar{\alpha}_s$. It follows from Eq. (29) that this is a limiting value of the parameter λ for the geometric scaling to hold asymptotically in the small x limit and so for $\lambda = 4\bar{\alpha}_s$ we expect violation of this scaling for $Q^2 > Q_s^2(x)$ down to very small values of x [20].

B. Running coupling case

We now pass to the more realistic case with running coupling. In this case the evolution equation for the moment function takes the form

$$\frac{\partial g_\omega(Q^2)}{\partial \ln(Q^2/\Lambda^2)} = \frac{\alpha_s(Q^2)}{2\pi} \gamma_{gg}(\omega) g_\omega(Q^2), \tag{30}$$

where the running coupling in leading order is given by

$$\frac{\alpha_s(Q^2)}{2\pi} = \frac{b}{\ln(Q^2/\Lambda^2)}, \tag{31}$$

with

$$b = \frac{2}{11 - 2/3 N_f}, \tag{32}$$

with N_f being the number of flavors. In this section we consider only the gluonic channel and therefore we set $N_f = 0$. The solution of Eq. (30) reads

$$g_\omega(Q^2) = g_0(\omega) \left(\frac{\ln(Q^2/\Lambda^2)}{\ln(Q_0^2/\Lambda^2)} \right)^{b\gamma_{gg}(\omega)}. \tag{33}$$

From the above solution we obtain

$$\frac{\alpha_s(Q^2)}{2\pi} g_\omega(Q^2) = \frac{\alpha_s(Q_0^2)}{2\pi} g_0(\omega) \left(\frac{\ln(Q^2/\Lambda^2)}{\ln(Q_0^2/\Lambda^2)} \right)^{b\gamma_{gg}(\omega)-1}, \tag{34}$$

and so the result for the gluon distribution $xg(x,Q^2)$ in x space reads in this case

$$\frac{\alpha_s(Q^2)}{2\pi} xg(x,Q^2) = \frac{1}{2\pi i} \int d\omega x^{-\omega} f_0(\omega) \left(\frac{\ln(Q^2/\Lambda^2)}{\ln(Q_0^2/\Lambda^2)} \right)^{b\gamma_{gg}(\omega)-1}, \tag{35}$$

where

$$f_0(\omega) = \frac{\alpha_s(Q_0^2)}{2\pi} g_0(\omega). \tag{36}$$

We now impose the geometric scaling condition (9) onto this solution to get

$$\frac{1}{2\pi i} \int d\omega x^{-\omega} f_0(\omega) \left(1 + \frac{\lambda \ln(1/x)}{\ln(Q_0^2/\Lambda^2)} \right)^{b\gamma_{gg}(\omega)-1} = r^0 x^{-\lambda}, \tag{37}$$

which is an equation for $f_0(\omega)$. Solution of this equation is complicated, i.e., the exact solution generates a complicated (branch point) singularity of $f_0(\omega)$ at $\omega = \lambda$. The only observation which we can make is that it should generate $x^{-\lambda}$ behavior softened by inverse powers of $\ln(1/x)$. In order to obtain some insight into what is going on we have to make some approximations. To be precise let us make the approximation by setting $\omega = \lambda$ in the argument of $\gamma_{gg}(\omega)$, which gives

$$\frac{1}{2\pi i} \int d\omega x^{-\omega} f_0(\omega) \simeq \left(1 + \frac{\lambda \ln(1/x)}{\ln(Q_0^2/\Lambda^2)} \right)^{-(b\gamma_{gg}(\lambda)-1)} r^0 x^{-\lambda}. \tag{38}$$

Making the same approximation in the inverse Mellin transform (35) we get the solution

$$\frac{\alpha_s(Q^2)}{2\pi} xg(x,Q^2) \simeq x^{-\lambda} r^0 \left(\frac{\ln(Q^2/\Lambda^2)}{\ln(Q_0^2/\Lambda^2)} \right)^{b\gamma_{gg}(\lambda)-1} \times \left(1 + \frac{\lambda \ln(1/x)}{\ln(Q_0^2/\Lambda^2)} \right)^{-(b\gamma_{gg}(\lambda)-1)}. \tag{39}$$

Multiplying and dividing Q^2 by $Q_0^2 x^{-\lambda}$ we finally obtain

$$\frac{\alpha_s(Q^2)}{2\pi} xg(x,Q^2) = x^{-\lambda} r^0 \left(\frac{\ln(Q^2 x^\lambda / Q_0^2)}{\ln(Q_0^2/\Lambda^2) + \lambda \ln(1/x)} + 1 \right)^{b\gamma_{gg}(\lambda)-1}. \tag{40}$$

The factor proportional to $\ln(1/x)$ in the denominator of the expression on the right-hand side (RHS) of Eq. (40) generates violation of the geometric scaling. Thus in the case of running of the coupling $\alpha_s(Q^2)$ the scaling behavior gets violated; it is possible, however, to factor out the effect of this violation. We can also rewrite Eq. (40) by using the definition of the saturation scale and the running coupling to get

$$\frac{\alpha_s(Q^2)}{2\pi} \frac{xg(x,Q^2)}{Q^2} = \frac{r^0}{Q_0^2} \frac{Q_s^2(x)}{Q^2} \left[1 + \frac{\alpha_s(Q_s^2(x))}{2\pi b} \ln[Q^2/Q_s^2(x)] \right]^{b\gamma_{gg}(\lambda)-1}, \tag{41}$$

where we see that the violation is proportional to the value of the running coupling evaluated at the saturation scale. Consequently, when $x \ll 1$, that is, when $Q_s(x) \gg 1$, the geometric scaling is restored, provided of course that $\alpha_s[Q_s^2(x)]\ln[Q^2/Q_s^2(x)] \ll 1$ as well. This condition is equivalent to $\ln[Q^2/Q_s^2(x)] \ll \ln[Q_s^2(x)/\Lambda^2]$. The same condition defining the region in which the geometric scaling holds above the saturation scale has recently been found in Ref. [25].

III. NUMERICAL RESULTS

In this section we present numerical results for the evolution of ordinary DGLAP equations for the integrated gluon distribution function with special boundary conditions set on the critical line $Q_s^2(x)$ as described in Sec. I.

A. Fixed coupling case

We start with the simplest case, which is the fixed strong coupling. We assume also in the first approximation the double leading-log approximation (DLLA) limit, that is, we only keep the most singular part of the P_{gg} splitting function in our simulation, i.e.,

$$P_{gg}(z) = \frac{2N_c}{z}, \quad N_c = 3, \tag{42}$$

which results in the following form for the anomalous dimension of Eq. (7):

$$\gamma_{gg}(\omega) = \frac{2N_c}{\omega}. \tag{43}$$

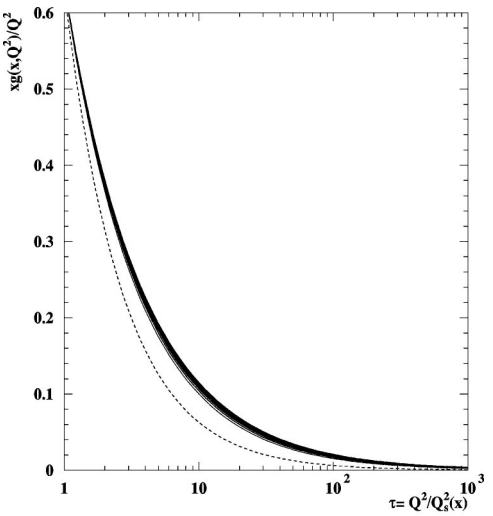

FIG. 2. Function $xg(x,Q^2)/Q^2$ in the DLLA fixed coupling case plotted versus scaling variable $\tau = Q^2/Q_s^2(x)$ for different values of rapidities $Y = \ln 1/x$, from $Y_{min} = 6.0$ to $Y_{max} = 46.0$ (solid curves from bottom to top) in steps $\Delta Y = 2$. Dashed curve is the input distribution $\sim 1/\tau$.

The initial condition for the evolution of the gluon density is assumed to be of the form (9). We take $\lambda = 0.5$ and $\alpha_s = 0.1$. In Fig. 2 we show the results of the calculation in this case. We illustrate the scaling behavior of the gluon density by plotting $xg(x,Q^2)/Q^2$ versus the scaling variable $\tau = Q^2/Q_s^2(x)$ for different values of rapidity $Y = \ln 1/x$. From Eq. (24) we see that this function should scale with $\tau = Q^2/Q_s^2(x)$. The geometric scaling would correspond in this plot (Fig. 2) to the perfect overlap of all curves for different values of Y, so that they would form one single line. We see that up to a good accuracy this function does not depend dramatically on Y and thus on x. We do however observe that there is some violation of the scaling at large x. This is due to the fact that the geometric scaling expression defined by Eq. (24) is only expected to hold asymptotically in the small x limit. At finite x this leading behavior is perturbed by the nonleading contribution given by the branch-point singularity of $\omega(z)$ at $z = 2\sqrt{\alpha_s}$ [see Eq. (26)].

To illustrate better the scaling and its violation we have plotted $xg(x,Q^2)/Q^2$ versus scaling variable $\tau = Q^2/Q_s^2(x)$ using a double-logarithmic scale [see Fig. 3(a)]. One clearly sees that with increasing rapidity Y the curves do not change and reach an asymptotic straight line. We have also selected the very low x range of Fig. 3(a), which is Fig. 3(b). One can see that in this case the geometric scaling is nearly preserved (we see nearly a single line for different rapidities).

The behavior of $xg(x,Q^2)/Q^2$ versus $\tau = Q^2/Q_s^2(x)$ is clearly governed by a power law, with a power which we estimate to be approximately -0.77. From Eqs. (24) and (28), and using the values of λ and α_s quoted above, we get that the power should be $(\alpha_s/2\pi)\gamma_{gg}(\omega_0) - 1 = -0.74$, which is in very good agreement with the numerical result.

Let us note that in the case of the DLLA Eq. (43) ω_0 is a solution of the quadratic equation and is given by Eq. (28). As previously noticed, the real solution exists only for λ

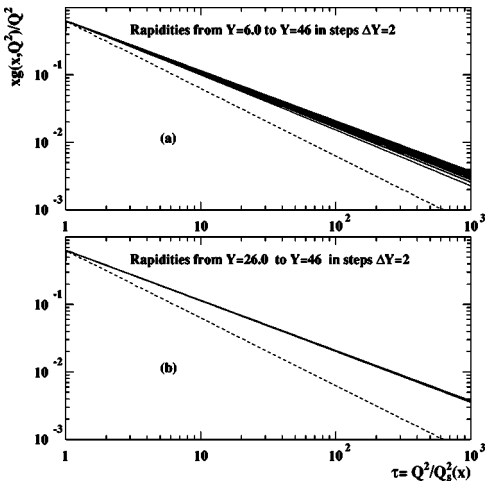

FIG. 3. Function $xg(x,Q^2)/Q^2$ in DLLA fixed coupling case plotted versus scaling variable $\tau=Q^2/Q_s^2(x)$ for different values of rapidities $Y=\ln 1/x$. Solid curves, solutions; dashed curve, input distribution $\sim 1/\tau$. On upper plot (a) solid curves from bottom to top are for Y rapidities ranging from $Y_{min}=6.0$ to $Y_{max}=46.0$ in steps $\Delta Y=2$. In lower plot (b) rapidities ranginge from $Y_{min}=26.0$ to $Y_{max}=46.0$ in steps $\Delta Y=2$.

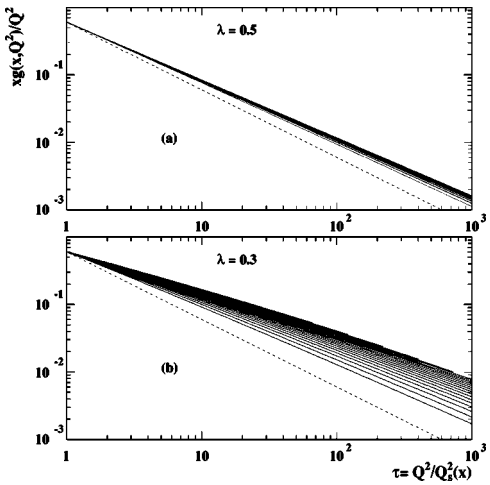

FIG. 4. Fixed coupling case with complete gluon anomalous dimension $\gamma_{gg}(\omega)$. Function $xg(x,Q^2)/Q^2$ plotted versus scaling variable $\tau=Q^2/Q_s^2(x)$ for different values of rapidities $Y=\ln 1/x$ from $Y_{min}=6.0$ to $Y_{max}=46.0$ in steps $\Delta Y=2$. Upper plot (a), scaling exponent $\lambda=0.5$; lower plot (b), scaling exponent $\lambda=0.3$.

$\geqslant\lambda_{min}=4\bar{\alpha}_s$ with $\bar{\alpha}_s=\alpha_s N_c/\pi$. We have numerically checked that for $\lambda\leqslant\lambda_{min}$ our solution no longer exhibits geometric scaling. It is interesting to note, as we have already observed at the end of Sec. II A, that exactly the same value of $\lambda=\lambda_{min}$ for a power of the saturation scale was obtained from the studies of the nonlinear Balitsky-Kovchegov equation [11,12] performed in [16–20].

We next abandon the DLLA and consider the more general case with the full gluon-gluon splitting function P_{gg} which gives the following anomalous dimension:

$$\gamma_{gg}(\omega)=2N_c\left[\frac{1}{\omega}-\frac{1}{\omega+1}+\frac{1}{\omega+2}-\frac{1}{\omega+3}-\gamma_E+\frac{11}{12}-\psi(\omega+2)\right], \tag{44}$$

where ψ is the Polygamma function. In this case Eq. (14) with $z=\lambda$ can no longer be solved analytically and has to be analyzed numerically. However, one can get insight into the allowed values of λ by making the expansion of the anomalous dimension around $\omega=0$. In this case $\gamma_{gg}(\omega)/(2N_c)\simeq 1/\omega+A_1(0)+\mathcal{O}(\omega)$ where $A_1(0)=-\frac{11}{12}$. Using this approximation in Eq. (14) one finds that now geometric scaling will hold if the following condition is satisfied:

$$\lambda\geqslant\lambda_{min}=\frac{4\bar{\alpha}_s}{[1-\bar{\alpha}_s A_1(0)]^2}. \tag{45}$$

We have checked numerically that the above approximation works very well and gives results very close to the solution of Eq. (14) with full ω dependence of the anomalous dimension $\gamma_{gg}(\omega)$.

In Fig. 4(a) we plot $xg(x,Q^2)/Q^2$ as a function of the scaling variable $Q^2/Q_s^2(x)$ in the case of calculation with the full anomalous dimension (44). We have taken $\lambda=0.5$ and $\bar{\alpha}_s=0.1$. We see that the function exhibits geometric scaling (although there is some residual violation at larger values of x). The calculated value of the exponent from numerical calculation is -0.85, which is again in nearly perfect agreement with the analytical estimate based on the approximation described above, which gives -0.86. We also present in Fig. 4b the calculation in the case of $\lambda=0.3$ which is below the critical value (45), equal in this case to $\lambda_{min}=0.33$ for $\bar{\alpha}_s=0.1$. We clearly see that the geometric scaling is never present in that case.

One can study the scaling and its violation in a more quantitative way by examining the following expression:

$$\Delta(Y,\tau)=\frac{1}{h}\frac{\partial h(Y,\tau)}{\partial Y}\bigg|_{\tau=\text{fixed}}, \tag{46}$$

where

$$h(Y,\tau)\equiv\frac{\bar{\alpha}_s}{Q^2}xg(x,Q^2). \tag{47}$$

The derivative $\Delta(Y,\tau)$ should vanish in the region where geometric scaling is satisfied. Consequently its deviation from zero will characterize the scaling violation of the solution (47).

We present the quantity $\Delta(Y,\tau)$ in Fig. 5 for the case of a calculation with complete anomalous dimension and two selected values of λ:0.3 and 0.5. The derivative $\Delta(Y,\tau)$ in Fig. 5 therefore illustrates the scaling and its violation for the solution shown in Fig. 4. From Fig. 5 it is clear that in $\lambda=0.5$ the scaling is always reached, even for high values of τ, which is very far right of the critical line. On the other hand, in the case $\lambda=0.3$ the derivative $\Delta(Y,\tau)$ never van-

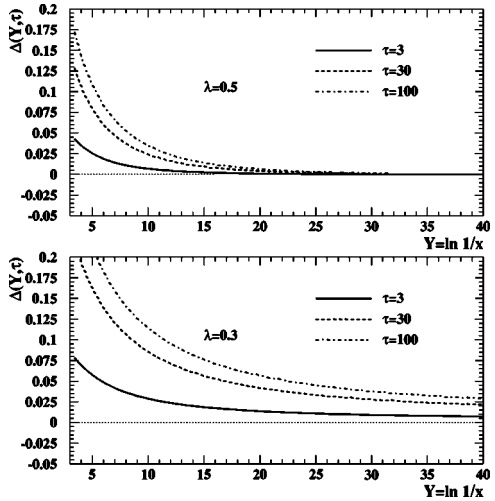

FIG. 5. The derivative $\Delta(Y,\tau)$ from Eq. (46) as a function of rapidity Y for various values of the scaling variable τ. Upper plot, scaling exponent $\lambda=0.5$; lower plot, scaling exponent $\lambda=0.3$.

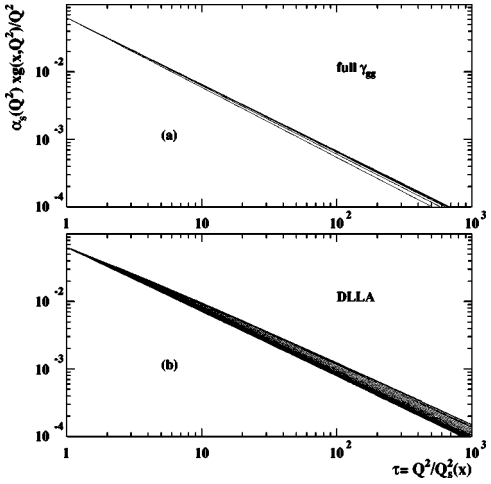

FIG. 6. The solution $\alpha_s(Q^2)xg(x,Q^2)/Q_s^2(x)$ in the running coupling case. Rapidity range from $Y_{min}=6.0$ to $Y_{max}=46.0$ in steps $\Delta Y=2$. Upper plot (a), case with full anomalous dimension $\gamma_{gg}(\omega)$; lower plot (b), case in DLLA approximation.

ishes, meaning that for $\lambda<\lambda_{min}$ the solution of the DGLAP equation in the fixed coupling case does not exhibit geometric scaling.

B. Running coupling case

We consider now the case in which α_s is running and study the impact of the scaling boundary condition (9) on the evolution. We consider the full expression for the anomalous dimension in that case, $\gamma_{gg}(\omega)$, given by Eq. (44). The running of the coupling requires that the evolution is taken in the region well above the Landau pole. In our case this means that one has to evolve with $Q^2>Q_s^2(x)$ and we would like to have $Q_s^2(x)$ big enough for all values of x. For the purpose of illustration we take $Q_s^2(x)=Q_0^2(x/x_0)^{-\lambda}$ where $Q_0^2=1.0$ GeV^2 and $x_0=1.0$. This means that at $x=1$ the saturation scale is $Q_s^2=1.0$ GeV^2. This assumption might seem artificial considering the present phenomenology of lepton-nucleon scattering, which suggests that the saturation scale could be of the order of 1 GeV^2 at $x\simeq 10^{-4}$ for the most central collisions at the HERA collider [22,26]. However, we use it here for the purpose of the illustration of basic effects of the evolution with special scaling boundary conditions. We concentrate here on presenting general properties of the solution rather than trying to describe the experimental data. We also take $N_f=0$, that is, we are considering the pure gluonic channel. In Fig. 6a we present the results of the calculation by plotting $\alpha_s(Q^2)xg(x,Q^2)/Q^2$ versus the scaling variable $\tau=Q^2/Q_s^2(x)$ in the case with a full gluon anomalous dimension. For comparison we also show the calculation performed in the DLLA (Fig. 6b). We see that the geometric scaling is mildly violated in the running coupling case, and more strongly in the DLLA due to the faster evolution. This fact can be understood on the basis of Eq. (41) where the numerical value of the exponent of expression on the RHS is much bigger in the DLLA case: $b\gamma_{gg}(\lambda=0.5)=0.18$ in the case with full anomalous dimension and $b\gamma_{gg}(\lambda=0.5)=13/11$ in the DLLA case.

We have tried to estimate whether the violation is consistent with the analytical prediction of formula (40). In Fig. 7a we present the same quantity as in Fig. 6a but multiplied by the scaling variable $\tau=Q^2/Q_s^2(x)$. The solid black curves in Fig. 7a from top to bottom are for decreasing values of x. One can see that the solution exhibits some small violation of the geometric scaling and that the magnitude of this violation is smaller for smaller values of x (the curves are becoming closer and closer as x decreases). This is consistent with the general behavior predicted by Eq. (40) where the scaling violating factor on the RHS tends to unity when $\ln(1/x)\gg 1$. We stress that the observed scaling violation is very small in this kinematical regime. For example, at a very high value of $\tau=10^3$ the violation of the scaling is about 5% in a huge rapidity range from $Y=6$ to $Y=46$.

It follows from Eqs. (40) and (41) that the violation of the geometric scaling can be approximately factored out. We checked this approximate prediction by considering the quantity

$$\alpha_s(Q^2)xg(x,Q^2)/Q_s^2(x)VF(x)$$

with

$$VF(x)=\left[\frac{\ln(Q^2/Q_s^2(x))}{\ln(Q_0^2/\Lambda^2)+\lambda\,\ln(1/x)}+1\right]^{1-b\gamma_{gg}(\lambda)} \tag{48}$$

which according to Eq. (40) should be constant with respect to $\tau=Q^2/Q_s^2(x)$. The results for the above quantity are shown in Fig. 7b [which is Fig. 7a multiplied by $VF(x)$] where now we see that the geometric scaling is approximately restored (the curves form a very narrow band) at high values of rapidity.

Also in the case of running coupling we have studied the features of the geometric scaling using the method of the derivative; see Eq. (46). The results are shown in Fig. 8 where it is clear that there is always a region where the geometric scaling is (approximately) preserved in the run-

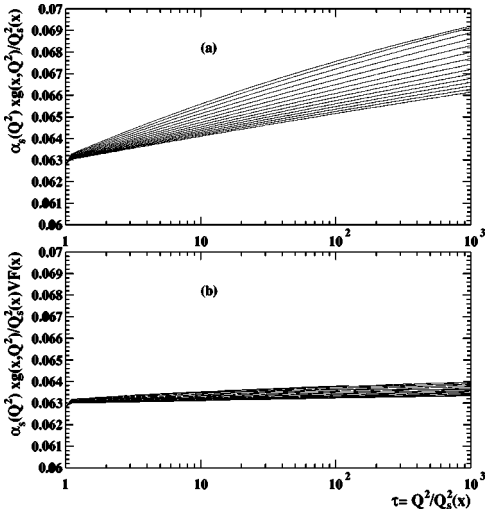

FIG. 7. The solution $\alpha_s(Q^2)xg(x,Q^2)/Q_s^2(x)$ in the running coupling case. We have selected the high rapidity range from $Y_{min}=18.0$ to $Y_{max}=46.0$ in steps $\Delta Y=2$. Upper plot (a), $\alpha_s(Q^2)xg(x,Q^2)/Q_s^2(x)$; lower plot (b), $\alpha_s(Q^2)xg(x,Q^2)/Q_s^2(x)VF(x)$ where the factor $VF(x)$ is a scaling violation factor defined in Eq. (48).

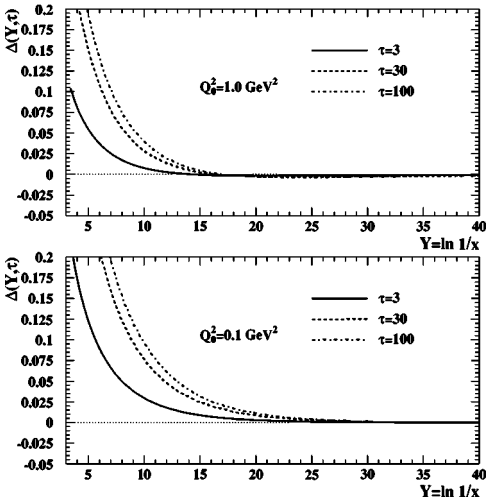

FIG. 8. The derivative $\Delta(Y,\tau)$ defined in Eq. (46) as a function of rapidity Y for different values of τ and different choices of normalization Q_0^2. The scaling exponent λ was set to be $\lambda=0.5$.

ning coupling case, even at very high values of τ. This is consistent with formula (41) provided we have $\bar{\alpha}_s(Q_s^2)\ln\tau \ll 1$ and $x \ll 1$, and also with the conclusions of Refs. [25,27]. We have also illustrated in Fig. 8 the sensitivity of the results to the variation of the normalization for the saturation scale, i.e., Q_0^2. Changing the parameter Q_0^2 from 1 (upper plot in Fig. 8) to 0.1 GeV^2 (lower plot in Fig. 8) influences the size of the violation of the scaling. One can see that the geometric scaling is postponed to higher values of rapidity.

IV. SUMMARY AND CONCLUSIONS

In this paper we studied the effects of the DGLAP evolution upon the geometric scaling. We solved the DGLAP evolution equation for the gluon distribution with the initial condition respecting the geometric scaling and provided along the critical line $Q^2=Q_s^2(x)$. In the case of fixed QCD coupling we obtained an analytic solution of the DGLAP equation with those boundary conditions, Eq. (21). We also showed that for sufficiently large values of the parameter λ defining the critical line this solution of the DGLAP equation preserves the geometric scaling for the leading term at small x [see Eq. (22)]. In the double-logarithmic approximation of the DGLAP equation this happens for $\lambda \geqslant 4\bar{\alpha}_s$, where $\bar{\alpha}_s$ is defined by Eq. (27). Geometric scaling is, however, violated by effects which are subleading at small values of x. We have also obtained an approximate solution of the DGLAP equation with the running coupling starting again from the boundary conditions respecting geometric scaling along the critical line. In the running coupling case geometric scaling is mildly violated for arbitrary values of the parameter λ, yet this violation can be approximately factored out. The size of this small violation is controlled by the quantity $\bar{\alpha}_s(Q_s^2)\ln Q^2/Q_s^2$. Thus in the region where $x \ll 1$ and $\ln Q^2/Q_s^2 \ll \ln Q_s^2/\Lambda^2$ the geometric scaling in the running coupling case is preserved. Results of the detailed numerical analysis confirmed all those expectations. We conclude that the geometric scaling is a very useful regularity following from the saturation model. We believe that it might be interesting to incorporate this ''DGLAP improved'' geometric scaling in the phenomenological analysis of the data.

ACKNOWLEDGMENTS

This research was partially supported by the EU Fourth Framework Program ''Training and Mobility of Researchers,'' Network ''Quantum Chromodynamics and the Deep Structure of Elementary Particles,'' contract FMRX-CT98-0194 and by the Polish Committee for Scientific Research (KBN), Grants No. 2P03B 05119, No. 2P03B 12019, and no. 5P03B 14420.

[1] L.V. Gribov, E.M. Levin, and M.G. Ryskin, Phys. Rep. **100**, 1 (1983).
[2] A.H. Mueller and J. Qiu, Nucl. Phys. **B268**, 427 (1986).
[3] A.H. Mueller, Nucl. Phys. **B415**, 373 (1994); A.H. Mueller and B. Patel, *ibid.* **B425**, 471 (1994); A.H. Mueller, *ibid.* **B437**, 107 (1995).
[4] A.H. Mueller, Nucl. Phys. **B335**, 115 (1990); Yu.A. Kovchegov, A.H. Mueller and S. Wallon, *ibid.* **B507**, 367 (1997); A.H. Mueller, Eur. Phys. J. A **1**, 19 (1998); Nucl. Phys. **A654**, 370 (1999); Nucl. Phys. **B558**, 285 (1999).
[5] J.C. Collins and J. Kwieciński, Nucl. Phys. **B335**, 89 (1990); J. Bartels, G.A. Schuler, and J. Blümlein, Z. Phys. C **50**, 91 (1991); Nucl. Phys. B (Proc. Suppl.) **18C**, 147 (1991).
[6] J. Bartels and E.M. Levin, Nucl. Phys. **B387**, 617 (1992).

[7] J. Bartels, Phys. Lett. B **298**, 204 (1993); Z. Phys. C **60**, 471 (1993); **62**, 425 (1994); J. Bartels and M. Wüsthoff, *ibid.* **66**, 157 (1995); J. Bartels and C. Ewerz, J. High Energy Phys. **09**, 026 (1999).

[8] L. McLerran and R. Venugopalan, Phys. Rev. D **49**, 2233 (1994); **49**, 3352 (1994); **50**, 2225 (1994); A. Kovner, L. McLerran, and H. Weigert, *ibid.* **52**, 6231 (1995); **52**, 3809 (1995); R. Venugopalan, Acta Phys. Pol. B **30**, 3731 (1999); E. Iancu and L. McLerran, Phys. Lett. B **510**, 145 (2001); L. McLerran, hep-ph/0104285; E. Iancu, A. Leonidov, and L. McLerran, Nucl. Phys. **A692**, 583 (2001); E. Ferreiro, E. Iancu, A. Leonidov, and L. McLerran, *ibid.* **A703**, 489 (2002); A. Capella *et al.*, Phys. Rev. D **63**, 054010 (2001).

[9] G.P. Salam, Nucl. Phys. **B449**, 589 (1995); **B461**, 512 (1996); Comput. Phys. Commun. **105**, 62 (1997); A.H. Mueller and G.P. Salam, Nucl. Phys. **B475**, 293 (1996).

[10] E. Gotsman, E.M. Levin, and U. Maor, Nucl. Phys. **B464**, 251 (1996); **B493**, 354 (1997); Phys. Lett. B **245**, 369 (1998); Eur. Phys. J. C **5**, 303 (1998); E. Gotsman, E.M. Levin, U. Maor, and E. Naftali, Nucl. Phys. **B539**, 535 (1999); A.L. Ayala Filho, M.B. Gay Ducati, and E.M. Levin, *ibid.* **B493**, 305 (1997); **B551**, 355 (1998); Eur. Phys. J. C **8**, 115 (1999).

[11] Ia. Balitsky, Nucl. Phys. **B463**, 99 (1996); I.I. Balitsky, Phys. Rev. Lett. **81**, 2024 (1998); Phys. Rev. D **60**, 014020 (1999); hep-ph/0101042; Phys. Lett. B **518**, 235 (2001).

[12] Yu.V. Kovchegov, Phys. Rev. D **60**, 034008 (1999); **61**, 074018 (2000).

[13] J. Jalilian-Marian, A. Kovner, L. McLerran, and H. Weigert, Phys. Rev. D **55**, 5414 (1997); J. Jalilian-Marian, A. Kovner, and H. Weigert, *ibid.* **59**, 014014 (1999); **59**, 014015 (1999); **59**, 034007 (1999); **59**, 099903(E) (1999); A. Kovner, J. Guilherme Milhano, and H. Weigert, *ibid.* **62**, 114005 (2000); H. Weigert, Nucl. Phys. **A703**, 823 (2002).

[14] M.A. Braun, Eur. Phys. J. C **16**, 337 (2000); hep-ph/0101070.

[15] Yu.V. Kovchegov and L. McLerran, Phys. Rev. D **60**, 054025 (1999); **62**, 019901(E) (2000); Yu.V. Kovchegov and E.M. Levin, Nucl. Phys. **B577**, 221 (2000).

[16] E.M. Levin and M. Lublinsky, Nucl. Phys. **A696**, 833 (2001); Eur. Phys. J. C **22**, 647 (2002).

[17] M. Lublinsky, Eur. Phys. J. C **21**, 513 (2001).

[18] N. Armesto and M.A. Braun, Eur. Phys. J. C **20**, 517 (2001); **22**, 351 (2001).

[19] E.M. Levin and K. Tuchin, Nucl. Phys. **B537**, 833 (2000); Nucl. Phys. **A691**, 779 (2001); **A693**, 787 (2001).

[20] K. Golec-Biernat, L. Motyka, and A.M. Staśto, Phys. Rev. D **65**, 074037 (2002).

[21] N.N. Nikolaev and B.G. Zakharov, Z. Phys. C **49**, 607 (1991); **53**, 331 (1992); **64**, 651 (1994); J. High Energy Phys. **08**, 598 (1994).

[22] K. Golec-Biernat and M. Wüsthoff, Phys. Rev. D **59**, 014017 (1998); **60**, 114023 (1999); Eur. Phys. J. C **20**, 313 (2001).

[23] J.R. Forshaw, G. Kerley, and G. Shaw, Phys. Rev. D **60**, 074012 (1999); hep-ph/007257.

[24] A.M. Staśto, K. Golec-Biernat, and J. Kwieciński, Phys. Rev. Lett. **86**, 596 (2001).

[25] E. Iancu, K. Itakura, and L. McLerran, hep-ph/0203137.

[26] S. Munier, A.M. Staśto, and A.H. Mueller, Nucl. Phys. **B603**, 427 (2001).

[27] A.H. Mueller and D.N. Triantafyllopoulos, hep-ph/0205167.